Received: Added at production | Revised: Added at production | Accepted: Added at production

DOI: xxx/xxxx

ARTICLE TYPE

An integrated planning framework for optimal power generation portfolio including frequency and reserve requirements

Olayinka Ayo[1] | **Paola Falugi**[1,2] | **Goran Strbac**[1]

[1]Department of Electrical and Electronic Engineering, Imperial College London, London, United Kingdom

[2]Department of Engineering & Construction, University of East London, London, United Kingdom

Correspondence
Corresponding author: Olayinka Ayo, Email: o.ayo17@imperial.ac.uk

Abstract

Electricity system decarbonisation poses several challenges to network stability and supply security, given renewables' intermittency and possible reduction of systems inertia. This manuscript presents a novel integrated system framework to determine optimal generation investments for addressing decarbonisation challenges and achieving cost-effective electricity systems while ensuring frequency stability and reserve requirements are met at operational level in a net-zero system. The novel planning framework is a mixed-integer bilinear programming problem accurately modelling clustered variables for on/off status of generation units and seconds-timescale frequency requirements at an operational and planning level. The benefits of the decision framework and effects of dispatch decisions in a year are illustrated using Great Britain case study. The results provide optimal trade-offs and cost-effective investment portfolios for including detailed modelling of unit-commitment and frequency stability constraints versus not including them in the planning model. Making investment decisions for a net-zero electricity system without these constraints can lead to very high system costs due to significant demand curtailment. Although the model's computation burden was increased by these constraints, complexity was managed by formulating them tightly and compactly. Non-convex quadratic nadir constraints were efficiently solvable to global optimality by applying McCormick relaxations and branching techniques in an advanced solver.

KEYWORDS
Power system planning, Unit commitment constraints, Frequency security constraints, Mixed-integer optimization, Spinning Reserves

1 | INTRODUCTION

The ambitious decarbonisation targets agreed upon by countries globally are bringing about significant transitions in technology investments and operations of power system networks. Achieving a low or net zero emission system requires substantial additions of variable, non-synchronous, low-carbon generators and the retirement of many conventional power plants[1,2,3]. In a bid to achieve supply security with variable and unpredictable renewable energy generators, enormous complexities are being imposed on the system. From the system operator perspective, the low inertia nature of a network with high penetration of intermittent renewable energy generators would require more reserves and flexibility to provide adequate frequency response and ancillary services[1,2,4,5]. Providing these services with conventional generators increases the chances of renewable power curtailment, especially during high output at off-peak times and in violation of emission targets, thereby increasing costs in the system. These challenges, therefore, highlight a need for cost-effective investment decisions in flexible technology solutions to attain supply security in future integrated low-carbon power systems. Whole system assessment of power systems networks has been shown to improve the cost-effectiveness of investments and operations of technologies[6 7].

Even though some authors[8] highlight that modelling unit commitment may not be relevant in a system with almost 100% renewables penetration, there are increasingly more flexible, clean firm technologies, such as hydrogen technologies, nuclear, biogas, and natural gas with carbon capture and

Abbreviations: Bn, Billion; CCGT, Combined cycle gas turbine; CCS, Carbon Capture and Storage; CUC, Clustered Unit Commitment; EFR, Enhanced Frequency Response; GB, Great Britain; GHR, Gas heated reformer; H, Hours; H_2, Hydrogen; H_2CCGT, Hydrogen combined cycle gas turbine; LHS, Left-hand side; M, Minutes; MIP, Mixed Integer Programming; MILP, Mixed Integer Linear Programming; NP, Nondeterministic Polynomial time; PFR, Primary Frequency Response; RHS, Right-hand side; RoCoF, Rate of change of frequency; UC, Unit commitment; Yr, Year.

storage (CCS) technology, necessary for reliability and balancing services in the future net-zero carbon electricity system[9]. Literature has shown that in a system with high penetration of variable renewable sources, modelling unit commitment (UC) constraints and online status of generators at the operational level are key for capturing the needed system flexibility, amongst other critical requirements like reserves and temporal constraints[10]. Some recent research works have shown the importance of operational details in an investment planning model[11]. However, only a few existing research studies have considered an integrated expansion planning problem of power systems, including detailed operational constraints, especially inter-temporal constraints like unit commitment, frequency, and reserve constraints. The few existing studies formulate the integrated expansion problem by adopting a considerably simplified description of the operational level. In a bid to highlight the benefits of unit commitment constraints modelling, Reference[11] showed hourly ramping rate constraints make for more cost-effective generation expansion decisions but excluded other relevant generator characteristics like the start-up/down cost or minimum-up & down time. However, such investment models do not adequately describe the value and potential of flexibility in power system technologies. References[12,13] emphasize the benefits of power-based unit-commitment modelling to accurately represent flexibility capabilities and system requirements, as they ensure more effective use of the installed generator investments when compared with an energy-based model. Specifically, Reference[14] highlighted that the tight and compact formulation of unit commitment, amongst the current state-of-the-art formulations, is more computationally efficient for solving day-ahead dispatch of generation units.

More so, References[13,15] proved that not including unit commitment constraints leads to overestimating the value and actual flexibility required from synchronous, renewable, and flexible technologies and underestimating the operational and total system cost. Neglecting UC constraints significantly affects the capacity mix deemed optimal by the model, the resulting generation mix, carbon emissions and cost projections, specifically for a highly renewable and carbon-constrained electricity system. This study focuses on capturing the operational flexibility of these more flexible power plants and flexible technologies in a planning model for accurate and cost-effective investments. Also, to replicate the ramping, reserve, startup/shutdown flexibility of individual unit commitment within a cluster, Reference[16] has proposed a more accurate method for formulating clustered power-based unit commitment, which will be adopted in this paper. The formulation includes constraints with binary on/off status and reserve assignment for individual units of clustered generators with identical technology to avoid overestimating their flexibility in a system with high penetration of variable renewable sources without increasing the computational burden.

Systems operators require flexibility to provide ancillary services, especially reserves and frequency response, balancing supply-demand deviations and essential system requirements in future power systems planning models. Increasingly, system operators need to procure more frequency response products like systems inertia, enhanced frequency response, and primary frequency response to handle the growing low inertia in the projected renewable energy-dominated system. A report by National Grid[17] proposed the need for sub-second, faster-acting response services from alternative technologies to conventional thermal plants to achieve optimum flexibility in power systems with decreasing inertia. The frequency response requirements on a system depend on the available system inertia and the size of the largest generator loss. Battery storage systems have been shown to provide the much-required sub-second response[17,18]. Through a novel frequency-constrained stochastic unit commitment model, Reference[19] further showed the benefits of co-optimizing energy production and provision of synchronized and synthetic inertia, Enhanced Frequency Response (EFR), Primary Frequency Response (PFR) and dynamically-reduced largest power in-feed. In addition, Reference[20] proved the capability of a Combined Cycle Gas Turbine Plant (CCGT) to provide the much-needed flexibility for future low-carbon power systems, especially those with enhanced flexibility parameters. Some studies have recognized the importance of including these frequency stability requirements in investment planning problems. Reference[21] in their article on assessing the impact of inertia and reactive power constraints in generation expansion planning, emphasized that disregarding inertia and reactive power constraints in generation expansion planning formulations can result in extra costs, load curtailment, and distortion of optimal resource allocation. However, their article did not consider the frequency stability constraints.

References[6,7] employed a whole system approach to determine the benefits of real-time balancing per second over a one-year time horizon. The model emphasized savings that can come from co-optimizing generation and network assets investment while improving the operational efficiency of different assets in the system. Frequency response and reserve provision from energy storage and conventional generators were considered without frequency-security constraints. In addition, reference[22] considered energy storage potential alongside conventional generators in the planning problem for primary frequency response adequacy and for improving the system's frequency security limits. This model did not consider the different response times of storage and conventional generators in providing frequency response. More specifically, these researches excluded detailed modelling of security constraints like the primary frequency response (PFR) constraints, which can ensure the security of supply at times of lower inertia and loss of the largest generator. Reference[8] showed that in unit commitment problems, the rate of change of frequency (RoCoF) limit is typically the most restrictive constraint in an inertia-aware binary unit commitment problem, compared to the limits on frequency nadir and quasi-steady state frequency deviation. Studying the impacts of omitting and including these other FR constraints in a generation planning problem becomes essential.

Reference[23] carried out studies on a planning problem, without detailed unit commitment modelling, to identify the role of the fast frequency response of energy storage systems and renewable technologies for ensuring frequency stability in future low inertia systems. The model included inertia and RoCoF contributions and showed some benefits, but inertia was fixed for different studies without considering the number of generators online. Similarly, reference[10] examined the impact of operational details on generation investment planning in a renewable energy-dominated system. The model included ramping limits, unit commitment and very fast frequency containment reserves requirements in inertia and RoCoF. However, apart from the integer unit commitment variable being relaxed to its linear counterpart, the research did not consider ramping costs, shutdown costs, or different start-up types. Also, the frequency stability constraints adapted did not consider load damping effect, nadir, or quasi-steady state requirements, and the largest generator loss was a fixed value as a function of time.

Whilst these studies have investigated some level of operational details in their power system models, the current study includes additional details for assessing the impact of scheduling and frequency stability constraints on investments in technologies. The paper reports a comparative study of integrated planning problems that consider different formulations of scheduling constraints. Both planning problems employ a clustered unit commitment formulation, but one of the formulations includes a detailed description of the commitment of the single generators.

2 | CONTRIBUTION AND APPROACH

This article proposes a novel integrated planning framework to determine the optimal technology portfolio for a cost-effective electricity system while ensuring frequency stability and reserve requirements at the operational level. The framework integrates the operational dynamics of post-fault frequency requirements[19] of the frequency rate of change, frequency nadir, and quasi-steady-state frequency in an integrated planning problem formulation selecting the optimal generation and flexible technologies portfolio. In order to meaningfully model the response limitations of conventional generators, we have adopted a detailed description of the inter-temporal constraints of each unit based on Reference[24]. The accurate unit commitment model allows considering simultaneous scheduling of multiple frequency services and identifying optimal investments in low carbon technologies like Hydrogen-powered CCGT (H_2CCGT), nuclear and renewable assets, as well as flexible technologies like battery storage, hydrogen storage and electrolysers, which operate at multiple timescales, for the security of supply and stable operation of future power systems. However, using an accurate unit commitment model in a planning problem, consisting of multiple investment options, services and timescales, gives rise to a challenging optimization problem due to the substantial increase of symmetries. As a result, additional constraints removing a large proportion of the symmetries have been introduced, to improve computational performances considerably. The resulting model is a large-scale mixed-integer bilinear programming problem solvable to global optimality by applying McCormick relaxations and spatial branching techniques implemented in Gurobi optimization solver[25].

To the best of the authors' knowledge, the proposed framework and relative case studies consider for the first time multiple post-fault seconds- timescale frequency requirements in an integrated planning problem formulation, including detailed descriptions of the inter-temporal constraints of each generator unit and contribution of different hydrogen and other flexible technologies for reserve and frequency provision services.

After applying the aforementioned linearisation techniques for bilinear constraints from using an advanced solver, the novel planning model becomes a mixed-integer linear programming problem optimised on a time horizon of one year and hourly time resolution consisting of discrete variables for investment costs and binary variables for the on/off status of generation units at the operational level. The presented deterministic studies focus on a cost-benefit system analysis capturing the effects of dispatch decisions in one year, from the central planner/utility point of view. The constraints formulated on the hourly variables include conditions happening on the time scales of seconds, especially for the frequency response requirements. Also, the requirements on an annual basis, like the need for hydrogen to be stored across seasons for periods of low renewable output, are formulated with estimated boundary conditions but still using the hourly time horizon. The benefits of the proposed approach are depicted through modelling and analyzing the technologies in a modified single-bus system to address some critical concerns about the role of storage and hydrogen technologies for the future power system. An extensive analysis of the impact of various system operational characteristics on generation expansion planning problems consisting of low-carbon conventional technologies, low-inertia renewable technologies, and flexible technologies has been performed to ensure system security and stability. The studies concurrently optimize investments in low-carbon technologies while minimizing the system's short-term operating costs through hourly time resolution representation of the system operation together with reserve and frequency stability and regulation requirements for a net-zero system. To the best of the authors' knowledge, the proposed study has not been conducted to the depth of modelling detail applied at the operations level of this planning problem.

A similar study was conducted by reference [10], where the impact of operational details on a single node generation investment planning in energy systems dominated by renewable plants was examined. However, apart from the integer unit commitment variable being relaxed to its linear counterpart, the analysis did not also consider ramping costs, shutdown costs or different start-up types. Also, the frequency stability constraints adopted did not consider load damping effect, nadir or quasi-steady state requirements. The largest generator loss was also considered to be a fixed value per time.

In summary, the main contributions of this paper are:

- We propose a model framework linking seconds-timescale frequency stability and hourly-timescale unit commitment to a yearly-timescale generation planning optimisation.
- We examined the impact of detailed seconds-timescale frequency stability and mixed integer unit commitment constraints, amongst other operational details, on optimal planning for investments in technologies simultaneously scheduled to provide inertia, primary frequency response, and enhanced frequency reserves in a net zero system.
- We also examined the integration of hydrogen technologies, especially H_2CCGT, for supporting frequency response, amongst other flexibility requirements.
- We propose additional constraints to remove a large proportion of the symmetries introduced by the clustered unit commitment variables to improve computational performances considerably.

All the studies consider the projected electricity and heating demand in the 2050 GB net-zero scenario developed by the government [1] to emphasize the impacts and benefits of considering frequency stability constraints in a generation expansion planning problem.

3 | PROBLEM FORMULATION

The proposed system design problem follows an integrated system approach to power planning according to [7,26] and captures the influence of fast dynamics at the investment temporal scale. The objective function to be minimized consists of the overall system costs (investment and operation cost) subject to investment and operation constraints:

$$\min_{x \in \mathcal{C}(\rho)} (V^I(x, \rho) + V^O(x, \rho)) \tag{1}$$

Equation (1) states both the investment cost function $V^I(\cdot)$ and operations cost function $V^O(\cdot)$ are to be minimised, where x denotes the whole collection of decision variables, ρ the system parameters and $\mathcal{C}(\cdot)$ the set of constraints depending on the parameters ρ. Refer to Appendix A for the nomenclature of the symbols used for the parameters and variables used in the problem formulation. The full set of constraints is introduced and discussed later in this section, while the investment cost function $V^I(\cdot)$ and operation cost function $V^O(\cdot)$ are as follows:

$$\begin{aligned} V^I(x, \rho) \quad &= \textstyle\sum_{n \in \Omega_N} (\sum_{s \in \Omega_S} \kappa_s^H H_{n,s} + \sum_{r \in \Omega_R^T} \kappa_r^G R_{n,r} \\ &+ \textstyle\sum_{g_T \in \Omega_G^T} \kappa_{g_T}^H G_{n,g_T} + \sum_{el \in \Omega_{EL}^T} \kappa_{el}^H G_{n,el}^H + \sum_{bl \in \Omega_{BL}^T} \kappa_{bl}^H G_{n,bl}^H) \end{aligned} \tag{2}$$

$$\begin{aligned} V^O(x, \rho) := \sum_{b \in \Omega_B} w_b \sum_{t \in \Omega_T^b} \Bigg\{ \Delta_t \Bigg[\sum_{g \in \Omega_G} (c_g^G (p_{t,g} + p_g^{msg} u_{t,g}) \\ + c_g^{nl} u_{t,g}) + \sum_{n \in \Omega_N} \Bigg[`\sigma_{t,n}^d + \sum_{s \in \Omega_S} (c_s^+ h_{t,n,s}^+ + c_s^- h_{t,n,s}^-) \Bigg] \Bigg] \\ + \sum_{n \in \Omega_N} (\sum_{el \in \Omega_{EL}^T} c_{el} Q_{t,n,el} + \sum_{bl \in \Omega_{BL}^T} c_{bl} Q_{t,n,bl}) + \sum_{g \in \Omega_G} c_g^{su} u_{t,g}^+ \\ + c_g^{sd} u_{t,g}^- + \Upsilon R_t^{slack} + \sum_{g \in \Omega_G} c_{res} res_{t,g} + \sum_{g \in \Omega_G} c_{rsp} rsp_{t,g} \Bigg\} \end{aligned} \tag{3}$$

The investment cost function $V^I(\cdot)$ deals with the balance among renewable generation, thermal generators, storage assets, hydrogen production technologies like gas-heated reformers with carbon capture storage (GHR-CCS), and electrolysers for blue and green hydrogen gas respectively. The storage assets include both battery storage and hydrogen storage plants. The operation cost function $V^O(\cdot)$ consists of the sum of generation cost, startup cost, no-load cost, shutdown cost, load curtailment, reserve curtailment, cost of reserve scheduling, [27], cost of hydrogen production, and storage operation costs. Load curtailment is economically penalized using the Value of Lost Load Γ, fixed at $30,000\$/MWh$, while reserve curtailment is economically penalized using Υ.

Limitations on investment in thermal generation technologies are as follows

$$0 \leq G_{n,g_T} \leq \overline{G}_{n,g_T}, \quad \forall g_T \in \Omega_G^T, \ \forall n \in \Omega_N \tag{4}$$

$$0 \leq G_{n,o}^H \leq \overline{G^H}_{n,o} \quad \forall o \in \Omega_{EL,BL}^T \ \forall n \in \Omega_N \tag{5}$$

Similar investment bounds have been imposed on other candidate technologies considered for investment in constraint(2).

Constraints (6) describe the supply-demand balance $\forall\, n \in \Omega_N$, $\forall\, t \in \Omega_T^b$ and $\forall b \in \Omega_B$

$$\begin{aligned} \sum_{g \in \Omega_G} J_{n,g} \left(p_{t,g} + p_g^{msg} u_{t,g} \right) + \sum_{r \in \Omega_R} p_{t,n,r}^R + \sum_{\ell \in \Omega_\ell} I_{n,\ell} f_{t,\ell} \\ + \textstyle\sum_{es \in \Omega_S^E} (h_{t,n,es}^- - h_{t,n,es}^+) + \sigma_{t,n}^d = d_{t,n} + \frac{Q_{t,n,el}}{\eta_{el}} \end{aligned} \tag{6}$$

In like manner, the supply-demand operation of the electrolyser, GHR-CCS hydrogen technology, and hydrogen storage technologies per time is described in constraint (7) $\forall b \in \Omega_B$, $\forall\, t \in \Omega_T^b - \{t_b^+\}$ [28]:

$$\sum_{n\in\Omega_N}\left(Q_{t,n,el} + Q_{t,n,bl} + \sum_{hs\in\Omega_S^H}(h^-_{t,n,hs} - h^+_{t,n,hs})\right) = \sum_{n\in\Omega_N}\left(J_{n,h2g}\frac{p_{t,h2g} + p^{msg}_{h2g}u_{t,h2g}}{\eta_{h2}}\right) \tag{7}$$

where $h2g$ indicates the H_2CCGT plants.

The LHS of supply-demand constraints (7) includes the sum of hydrogen produced by the electrolyser, GHR-CCS, and hydrogen stored, while the RHS describes the demand for hydrogen driven by the electrical power output of the H_2CCGT plant. Note that in constraint (7), hydrogen transportation is neglected as the balance is performed by summing over all the bus nodes. The operation of the hydrogen production by electrolyser and GHR-CCS is modelled as follows $\forall b \in \Omega_B$, $\forall\, t \in \Omega_T^b - \{t_b^+\}$ [28]:

$$0 \le Q_{t,n,el} \le G^H_{n,el} \quad \forall el \in \Omega^T_{EL}\ \forall n \in \Omega_N \tag{8}$$

$$0 \le Q_{t,n,bl} \le G^H_{n,bl} \quad \forall bl \in \Omega^T_{BL}\ \forall n \in \Omega_N \tag{9}$$

Constraints (8) and (9) describe the operational boundaries of the hydrogen produced by electrolyser and GHR-CCS, respectively.

The limits and distribution of the power flow over the network are described by the following constraints $\forall b \in \Omega_B$, $\forall t \in \Omega_T^b$, and $\forall \ell \in \Omega_\ell$

$$f_{t,\ell} = \frac{1}{\varkappa_\ell}\left(\theta_{t,w_\ell} - \theta_{t,v_\ell}\right), \quad \left|f_{t,\ell}\right| \le F^0_\ell. \tag{10}$$

In this model, the line capacity for providing reserves is assumed to be available, and enough room is left in the lines for its provision. The provision of reserves is doubled based on the need to satisfy flow conditions and reserve provisions from different nodes.

3.1 | Storage operation

The storage operation is modelled as follows $\forall b \in \Omega_B$, $\forall\, t \in \Omega_T^b$ $\forall s \in \Omega_S$ and $\forall n \in \Omega_N$.

$$\tilde{h}_{t+1,n,s} = \tilde{h}_{t,n,s} + \Delta_t(\rho_s^+ h^+_{t,n,s} - \frac{h^-_{t,n,s}}{\rho_s^-}) \tag{11}$$

$$\tilde{h}_{t_b^+,n,s} = \tilde{h}_{t_b^-+1,n,s} \tag{12}$$

$$0 \le h^-_{t,n,s} \le \hat{S}^-_{n,s} := \overline{S}_{n,s}\overline{h}_s + H^n_{0,s} \tag{13}$$

$$0 \le h^+_{t,n,s} \le \hat{S}^+_{n,s} := \overline{S}_{n,s}\overline{h}_s + H^n_{0,s} \tag{14}$$

$$0 \le \tilde{h}_{t,n,s} \le \hat{Z}_{n,s} := \overline{S}_{n,s}\overline{\eta}_s + \hat{Z}^n_{0,s} \tag{15}$$

where $H^n_{0,s}$, $H^n_{0,s}$ and $\hat{Z}^n_{0,s}$ describe the existing storage technology s at bus n. Constraint (11) computes the energy level of the storage for each time period. Constraint (12) assigns the energy level at the beginning of a block equal to the value at its end. The convex formulation of the storage constraints include charge and discharge efficiency parameters (ρ_s^+, ρ_s^-) which have values less than 100%. Since the efficiency value is less than one, there will be energy losses while cycling, limiting the occurrence of simultaneous charging and discharging [29]. In addition, a small cost of charging and discharging introduced in the objective function (2) has been introduced in the model as a penalty parameter [29]. Since the model considers losses and charging and discharging operation costs, the solutions with simultaneous charging and discharging are not optimal. Since hydrogen storage is seasonal, its behaviour follows an annual periodicity. It requires assigning the energy level at the beginning of the year equal to the energy level at the end of the year. Constraint (13 - 15) describes the limits on the charge, discharge, and energy level variables of the storage. To determine the initial storage condition for each temporal block and impose periodic annual conditions, we introduce a dynamic equation describing the energy accumulated or used during the year as follows:

$$\tilde{z}_{b+1,n,hs} = \tilde{z}_{b,n,hs} + w_b \sum_{t\in\Omega_T^b}(\Delta_t(\rho^+_{hs}h^+_{t,n,hs} - \frac{h^-_{t,n,hs}}{\rho^-_{hs}})), \tag{16}$$

$$\tilde{z}_{1,n,hs} = \tilde{z}_{N_b+1,n,hs} \tag{17}$$

for temporal blocks $b = 1, \ldots, N_b + 1$. Constraints (16) estimate the energy level for each temporal block from the daily difference of total charge and discharge variables while constraint (17) is similar to constraint (12) but applied to the first temporal block in the year and the first time block in the next year. The initial conditions for hydrogen storage are then defined by

$$\tilde{h}_{t_b^+,n,hs} = \tilde{z}_{b,n,hs}, \quad \forall b \in \Omega_b \tag{18}$$

Constraint (18) ensures that the energy level at the start of the day in a temporal block is equivalent to the total energy level at the beginning of its temporal block.

3.2 | Generator scheduling constraints

To represent the ability of different generation technology to provide frequency services, we need to take into account ramping limits, and for this reason, we model the on/off status of each thermal generation unit. Aggregate models of thermal generators do not accurately identify the ramping capability of the system because a feasible solution of the aggregate model does not imply the existence of a feasible solution for the current operating condition of every single generator. The integer unit commitment formulation proposed in [16,24,30] has numerical advantages since the model is almost tight when the integrality constraints are relaxed. The thermal generators are required to satisfy minimum up/down times and logical constraints

$\forall b \in \Omega_B, \forall t \in \Omega_T^b - \{t_b^+\}, \forall g \in \Omega_G$:

$$u_{t,g} - u_{t-1,g} = u_{t,g}^+ - u_{t,g}^-, \quad u_{t,g}, u_{t,g}^+, u_{t,g}^- \in \{0, 1, \ldots, N_g\} \quad (19)$$

$$\sum_{k=t-\hat{T}_g^U+1}^{t} u_{k,g}^+ \leq u_{t,g} \quad \forall t \geq \hat{T}_g^U + t_b^+ - 1 \quad (20)$$

$$\sum_{k=t-\hat{T}_g^D+1}^{t} u_{k,g}^- \leq N_g - u_{t,g} \quad \forall t \geq \hat{T}_g^D + t_b^+ - 1 \quad (21)$$

Logical constraint (19) represents the equation which guarantees the start-up variable $u_{t,g}^+$ and shut-down variable $u_{t,g}^-$ take the appropriate values when the generator units are online and offline[24]. Constraints (20) and (21) guarantee the minimum periods for which the units must be online and offline, where $\hat{T}_g^U$ and $\hat{T}_g^D$ represent the scaled number of hours that the generator units are online and offline, respectively. Assuming uniform sampling in demand blocks, $\hat{T}_g^U := \lceil T_g^{mu} \div \Delta_t \lceil$ and $\hat{T}_g^D := \lceil T_g^{md} \div \Delta_t \lceil$ where $\lceil \cdot \lceil$ denotes the ceiling function that gives as output the least integer equal or greater than the value of its argument. The generation limits are as follows ([24,30]) $\forall b \in \Omega_B, \forall t \in \Omega_T^b, \forall g \in \Omega_G$

if $T_g^{mu} \geq 2$

$$\begin{aligned} 0 \leq p_{t,g} + rsp_{t,g} + res_{t,g} \leq (\overline{P}_g - p_g^{msg})u_{t,g} \\ -(\overline{P}_g - SU_g)u_{t,g}^+ - (\overline{P}_g - SD_g)u_{t+1,g}^- \end{aligned} \quad (22)$$

if $T_g^{mu} = 1$,

$$\begin{aligned} 0 \leq p_{t,g} + rsp_{t,g} + res_{t,g} \leq (\overline{P}_g - p_g^{msg})u_{t,g} \\ -(\overline{P}_g - SU_g)u_{t,g}^+ - max(SU_g - SD_g, 0)u_{t+1,g}^- \end{aligned} \quad (23)$$

$$\begin{aligned} 0 \leq p_{t,g} + rsp_{t,g} + res_{t,g} \leq (\overline{P}_g - p_g^{msg})u_{t,g} \\ -max(SD_g - SU_g, 0)u_{t,g}^+ - (\overline{P}_g - SD_g)u_{t+1,g}^- \end{aligned} \quad (24)$$

where cyclic boundary conditions $u_{t_b^-,g}^- = u_{t_b^+,g}^-$ are enforced $\forall b \in \Omega_B$ and $\forall g \in \Omega_G$. The generation limit equations include the power output $p_{t,g}$, spinning reserve $res_{t,g}$ and frequency response $rsp_{t,g}$ contributions of the clustered units. Constraints (23) and (24) only apply for the subset of clustered generator units with $T_g^{mu} = 1$, while constraint (22) is for the subset of generators with $T_g^{mu} \geq 2$. Reference[24] emphasizes that constraint (22) is much tighter and compact than constraints (23) and (24). To impose that candidate generators can operate only if the necessary investment has taken place, we model linear constraints linking the operation of candidate generators g to the integer investment G_{n,g_T}[13]. In particular, the proposed constraints impose that the variables $u_{t,g}$, $u_{t,g}^+$, $u_{t,g}^-$ can assume non-zero values only if the cluster g has been built. For all $b \in \Omega_B$, $\forall t \in \Omega_T^b$ and $g \in \Omega_N \times \Omega_G^T$ the following constraints,

$$u_{t,g} \leq G_{n,g_T}, \; u_{t,g}^+ \leq G_{n,g_T}, u_{t,g}^- \leq G_{n,g_T}. \quad (25)$$

guarantee that aggregate generators can be active only if the relative investment occurs.

The operating initial conditions of the generator units at time t-1, which considers the previous state of the units, are imposed in this model. The system's initial condition depends on the operating conditions at the end of the demand period, given each demand block represents a typical period in the year. The conditions are as follows:

$$u_{t_b^+,g} - u_{t_b^-,g} = u_{t_b^+,g}^+ - u_{t_b^+,g}^-, \quad (26)$$

$$\sum_{k=\hat{t}_b^- - \hat{T}_g^U + 1 + t}^{\hat{t}_b^-} u_{k,g}^+ + \sum_{k=\hat{t}_b^+}^{t} u_{k,g}^+ \leq u_{t,g} \quad \forall \hat{t}_b^+ \leq t \leq \hat{T}_g^U + t_b^+ - 1 \quad (27)$$

$$\sum_{k=\hat{t}_b^- - \hat{T}_g^D + 1 + t}^{\hat{t}_b^-} u_{k,g}^- + \sum_{k=\hat{t}_b^+}^{t} u_{k,g}^- \leq N_g - u_{t,g} \quad \forall t_b^+ \leq t \leq \hat{T}_g^D + t_b^+ - 1 \quad (28)$$

The total power produced by the cluster $g \in \Omega_N \times \Omega_G^T$ is expressed as the sum of two terms as follows

$$P_{t,g} = p_g^{msg} u_{t,g} + p_{t,g} \quad \forall t, g. \quad (29)$$

The first term describes the unit's minimum stable generation and the second one is the additional generation output over the minimum. Total commitment, frequency response, spinning reserve and production output of the clustered units, which sums up the contributions from individual generator units, are given by:

$$u_{t,g} = \sum_{i \in \Omega_I^g} \tilde{u}_{t,g,i} \quad \forall t, g \quad (30)$$

$$rsp_{t,g} = \sum_{i \in \Omega_I^g} r\tilde{s}p_{t,g,i} \quad \forall t, g \quad (31)$$

$$res_{t,g} = \sum_{i \in \Omega_I^g} r\tilde{e}s_{t,g,i} \quad \forall t, g \quad (32)$$

$$p_{t,g} = \sum_{i \in \Omega_I^g} \tilde{p}_{t,g,i} \quad \forall t, g \quad (33)$$

The computation of constraints (30 - 33 are based on the need to model the individual ramping constraints of generators in the clustered unit to avoid the overestimation of their ramping and reserve flexibility[16]. A commitment order in every cluster is enforced $\forall t, g$ to remove multiple equivalent solutions as follows:

$$\tilde{u}_{t,g,1} \leq 1 \quad (34)$$

$$\tilde{u}_{t,g,i+1} \leq \tilde{u}_{t,g,i} \quad \forall i = 2, \ldots, Ng - 1 \quad (35)$$

$$\tilde{u}_{t,g,N_g} \geq 0 \quad (36)$$

$$\begin{aligned} \tilde{p}_{t,g,i+1} + r\tilde{s}p_{t,g,i+1} + r\tilde{e}s_{t,g,i+1} \leq \\ \tilde{p}_{t,g,i} + r\tilde{s}p_{t,g,i} + r\tilde{e}s_{t,g,i} \quad \forall i = 1, \ldots, Ng - 1 \end{aligned} \quad (37)$$

Constraints (34) to (36) have been modelled according to Reference[16] to ensure the successive order of commitment of the units starting from unit 1, while constraint (37) is introduced to ensure symmetries in the generators' model are removed, and the production of individual units are limited. The model which properly estimates the startup and shutdown capabilities for the individual generator units i is as shown in constraints (38 - 40) $\forall\, t, g, i = 1, \ldots, Ng$:

if $T_g^{mu} \geq 2$:

$$\tilde{p}_{t,g,i} + \tilde{rsp}_{t,g,i} + \tilde{res}_{t,g,i} \leq (SU_g - p_g^{msg})\tilde{u}_{t,g,i} + (\overline{P}_g - SU_g)\tilde{u}_{t-1,g,i} \quad \forall\, t, g, i = 1, \ldots, Ng \tag{38}$$

$$\tilde{p}_{t,g,i} + \tilde{rsp}_{t,g,i} + \tilde{res}_{t,g,i} \leq (SD_g - p_g^{msg})\tilde{u}_{t,g,i} + (\overline{P}_g - SD_g)\tilde{u}_{t+1,g,i} \quad \forall\, t, g, i = 1, \ldots, Ng \tag{39}$$

and if $T_g^{mu} = 1$:

$$\tilde{p}_{t,g,i} + \tilde{rsp}_{t,g,i} + \tilde{res}_{t,g,i} \leq (SU_g - \overline{P}_g + SD_g - p_g^{msg})\tilde{u}_{t,g,i} + (\overline{P}_g - SU_g)\tilde{u}_{t-1,g,i} + (\overline{P}_g - SD_g)\tilde{u}_{t+1,g,i} \tag{40}$$

The ramping limits for the individual units are guaranteed with the following constraints $\forall\, t, g, i = 1, \ldots, Ng$:

$$\tilde{p}_{t,g,i} - \tilde{p}_{t-1,g,i} + \tilde{rsp}_{t,g,i} + \tilde{res}_{t,g,i} \leq RU_g \Delta_t \tilde{u}_{t,g,i} \tag{41}$$

$$\tilde{p}_{t-1,g,i} - \tilde{p}_{t,g,i} \leq RD_g \Delta_t \tilde{u}_{t-1,g,i} \tag{42}$$

In addition, the present model includes fast reserves for frequency response and spinning reserves. Thermal generators and storage devices can all contribute to the achievement of the system frequency response and reserve requirements $\forall b \in \Omega_B$, $\forall\, t \in \Omega_T^b$:

$$\sum_{g\in\Omega_G} \sum_{i\in\Omega_I^g} \tilde{rsp}_{t,g,i} + \sum_{n\in\Omega_N} (\sum_{es\in\Omega_S^E} \hat{\alpha}_{t,n,es}^{rsp} \geq P_t^L - R_t^{slack} \tag{43}$$

$$\sum_{g\in\Omega_G} \sum_{i\in\Omega_I^g} \tilde{res}_{t,g,i} + \sum_{n\in\Omega_N} \left\{\sum_{es\in\Omega_S^E} \hat{\alpha}_{t,n,es}^{res}\right\} \geq Res_t^{min} - R_t^{slack}. \tag{44}$$

Constraints (43) and (44) ensure adequate contributions from the thermal generators and storage devices for meeting the minimum frequency response and spinning reserves, respectively, where the minimum reserves requirement are given by,

$$Res_t^{min} = 0.1 \left\{ \sum_{n\in\Omega_N} (d_{t,n} + \sum_{r\in\Omega_R} p_{t,n,r}^R) \right\} \tag{45}$$

The spinning reserve requirements depend on uncertainty or forecast error in intermittent generation and demand. All the generation and storage contributions $rsp_{t,g}$, $\hat{\alpha}_{t,n,es}^{res}$ and $\hat{\alpha}_{t,n,es}^{rsp}$ are subject to physical limitations $\forall b \in \Omega_B$, $\forall\, t \in \Omega_T^b$, $\forall\, es \in \Omega^S$

$$0 \leq \hat{\alpha}_{t,n,es}^{rsp} \leq \overline{Rsp}_{es} := P_L^{max},\ 0 \leq \hat{\alpha}_{t,n,es}^{res} \leq \overline{Res}_{es} \tag{46}$$

$$(\hat{\alpha}_{t,n,es}^{res} + \hat{\alpha}_{t,n,es}^{rsp}) \leq \hat{S}_{es}^{-} - h_{t,n,es}^{-} + h_{t,n,es}^{+} \tag{47}$$

$$(N_{es}^{rsp} \hat{\alpha}_{t,n,es}^{rsp} + N_{es}^{res} \hat{\alpha}_{t,n,es}^{res}) \leq \tilde{h}_{t,n,es} \tag{48}$$

$$0 \leq \tilde{rsp}_{t,g,i} \leq \tilde{u}_{t,g,i} \overline{Rsp}_g \tag{49}$$

where $\overline{Rsp}_g$ and $\overline{Rsp}_{es}$ are the maximum frequency response capabilities of a generation unit in the cluster g and of storage es, respectively. The parameters N_{es}^{res} and N_{es}^{rsp} refer to the time, storage s must provide the slow and fast response, respectively. The power output of intermittent sources satisfies, $\forall b \in \Omega_B$, $\forall\, t \in \Omega_T^b$, $\forall n \in \Omega_N$ and $\forall r \in \Omega_R$,

$$0 \leq p_{t,n,r}^R \leq \xi_{t,r,n}(R_{n,r} + R_{r,n}^0) \tag{50}$$

where $R_{n,r}$ is the capacity size (MW) of candidate renewable installations, $R_{r,n}^0$ represents the existing capacity and $\xi_r(t)$ is the performance factor of technology r at time t.

The carbon emissions of a thermal unit in the cluster g at time t can be modelled as a linear function of the generated power and the annual carbon limits as follows:

$$\sum_{b\in\Omega_B} w_b (\sum_{g\in\Omega_G} \sum_{t\in\Omega_T} (a_g^V \Delta_t (p_{t,g} + p_g^{msg} u_{t,g}) + a_g^{NL} u_{t,g} + a_g^{UP} u_{t,g}^{+})) \leq \sum_{b\in\Omega_B} w_b \sum_{n\in\Omega_N} \sum_{t\in\Omega_T^b} (E^T d_{t,n}) \tag{51}$$

where a_g^V (kg/MWh) is the variable emission coefficient of the cluster g, a_g^{NL} $(kgCO2)$ the no load emission coefficient and a_g^{UP} $(kgCO2)$ the start-up load emission coefficient. The adopted unit commitment formulation, presented in this section, combining constraints on the aggregates and single generators, ensures quality and faster solutions and reduces computational burden compared to using either classic clustered or binary unit commitment formulation alone[16]. Apart from reducing computational burden, the proposed modelling technique accurately evaluates the flexibility provided by every single generator when considering frequency response constraints.

3.3 | Frequency response constraints

The proposed model, similar to[19], combines the new FR service, EFR, recently introduced by National Grid in Great Britain, which should deliver responses within one second, together with primary frequency response services from available conventional generators delivered in less than ten seconds. The analysis of the swing equation, describing the time evolution of frequency deviation after a generation outage, allows the identification of constraints guaranteeing the satisfaction of the dynamic frequency requirements. The swing equation (52) describes the frequency dynamic as a function of the time τ immediately after a generation outage P_t^L occurs at time t[19]:

$$\frac{2H_t}{f_o}\frac{d\Delta f(\tau)}{d\tau} + D\, P_t^D\, \Delta f(\tau) = \sum_{es\in\Omega_S^E} EFR_{t,es}(\tau) + \sum_{g\in\Omega_G^T} PFR_{t,g}(\tau) - P_t^L \tag{52}$$

where

$$EFR_{t,es}(\tau) = \begin{cases} R_{t,es}^{ES}\tau/T^{es} & \text{if } \tau \leq T^{es} \\ R_{t,es}^{ES} & \text{if } \tau > T^{es} \end{cases} \tag{53}$$

$$PFR_{t,g}(\tau) = \begin{cases} R_{t,g}^{G}\tau/T^{G} & \text{if } \tau \leq T^{G} \\ R_{t,g}^{G} & \text{if } \tau > T^{G} \end{cases} \tag{54}$$

The largest power in-feed P_t^L satisfies $\forall b \in \Omega_B$, $\forall t \in \Omega_T^b$

$$\tilde{p}_{t,g,i} + p_g^{msg} \tilde{u}_{t,g,i} \leq P_t^L \leq P_L^{max}, \quad \forall\, g \in \Omega_G, i = 1, \ldots, Ng \tag{55}$$

$$\Psi \leq P_t^L \leq P_L^{max} \quad \forall\, r \in \Omega_R,\ \forall n \in \Omega_N \tag{56}$$

Where Ψ is a parameter to be chosen by the planner to take into account other losses that are relevant, like the loss of a wind farm of a certain size. The definition of P_t^L as a decision variable $\forall b \in \Omega_B$ and $\forall t \in \Omega_T^b$ is advantageous because dynamically choosing the largest power infeed reduces the maximum potential RoCoF after a generator loss, as supported by[31]. This approach is more efficient than increasing the inertia levels in the system through the addition of synchronous generators, as it would not be a long-term economical solution, given the decreasing system inertia due to renewable integration.

The highest value for the RoCoF occurs at $\tau = 0$ and the RoCoF security constraint[19] at the instant of outage $\forall b \in \Omega_B$, $\forall t \in \Omega_T^b$ is

$$0 \leq \frac{P_t^L f_0}{2 H_t} \leq \overline{RoCoF} \tag{57}$$

Note that condition (57) guarantees that $\Delta f(\tau)$ cannot become smaller than Δf_{max} = –0.8Hz before $\hat{\tau} = 0.8/RoCoF_{\max}$ = 1.6s. This implies that a minimum of $\Delta f(\tau)$ occurring at values $\tau \leq \hat{\tau}$ does not correspond to a critical situation. For this reason, we will consider only the minimum sitting in the interval $[T_{es}, T_g]$ since in our case studies $T_{es} < \hat{\tau}$.

The system inertia level after the largest generator loss is

$$H_t = \sum_{g \in \Omega_G} \sum_{i \in \Omega_I^g} H_g \overline{P}_g \tilde{u}_{t,g,i} - H_t^{Loss} \tag{58}$$

$$P_g^{max,L} H_g^L \tilde{u}_{t,g,i} \leq H_t^{Loss} \quad \forall g \in \Omega_G, \forall i \tag{59}$$

$$\delta \leq H_t \tag{60}$$

where $P_g^{max,L}$ is the size of the largest generator and δ is a constant parameter satisfying $0 < \delta \leq \min_{g \in \Omega_G} H_g \overline{P}_g$. The condition in (59) ensures considering the most significant possible inertia level loss H_t^{Loss} at every time, while (60) requires the existence of at least a conventional generator online. Constraint (60) models the minimum requirement for system inertia, a key consideration proposed in a system with high penetration of variable renewable technologies[32,33].

To ensure the achievement of quasi-steady-state security, we impose the following constraint $\forall b \in \Omega_B$, $\forall t \in \Omega_T^b$

$$\frac{P_t^L - R_t^{ES} - R_t^G}{D P_t^D} \leq \Delta f_{max}^{ss}, \tag{61}$$

where the total EFR, R_t^{ES}, satisfies

$$R_t^{ES} := \sum_{es \in \Omega_S^E} R_{t,es}^{ES} = \sum_{n \in \Omega_N} \sum_{es \in \Omega_S^E} \hat{\omega}_{t,n,es}^{rsp} \tag{62}$$

where

$$\hat{\omega}_{t,n,es}^{rsp} \leq \hat{\alpha}_{t,n,es}^{rsp} \tag{63}$$

The introduction of $\hat{\omega}_{t,n,es}^{rsp}$ allows for flexibility in the actual amount of frequency response that can be allocated by energy storage, where $\hat{\alpha}_{t,n,es}^{rsp}$ is the maximum allocated.

The total PFR, R_t^G, is such that

$$R_t^G := \sum_{g \in \Omega_G} R_{t,g}^G = \sum_{g \in \Omega_G} \sum_{i \in \Omega_I^g} r\tilde{s}p_{t,g,i} \leq \sum_{g \in \Omega_G} \sum_{i \in \Omega_I^g} \overline{Rsp}_g \tilde{u}_{t,g,i} \tag{64}$$

it is also required:

$$R_t^G \geq \underline{R}^G := \min_{g \in \Omega_G} \overline{RSP}_g \tag{65}$$

Based on the analysis performed in[19], the following quadratic expression accounts for the frequency nadir requirements.

$$\begin{aligned}\left(\frac{H_t}{f_0} - \frac{R_t^{ES}\, T^{es}}{4\,\Delta f_{max}}\right) R_t^G \geq \frac{(P_t^L - R_t^{ES})^2 T^G}{4\,\Delta f_{max}} \\ - \frac{(P_t^L - R_t^{ES})\, T^G D}{4} P_t^D\end{aligned} \tag{66}$$

Note that constraint (66) takes into account the effect of damping, and its good approximation properties are discussed in[19].

Moreover, since the nadir frequency occurs at time $t' \in [0, T_g]$, the following constraints have been included $\forall b \in \Omega_B$, $\forall t \in \Omega_T^b$,

$$P_t^L - R_t^{ES} - D\, P_t^D\, |\Delta f_{nadir}| \geq 0 \tag{67}$$

$$P_t^L - R_t^{ES} - D\, P_t^D\, |\Delta f_{nadir}| \leq R_t^G \tag{68}$$

to ensure the requirements are met within the response time of the frequency response services. The quadratic expression for the nadir constraint (66) is non-convex. Consequently, the resulting model is a mixed integer quadratic programming (MIQP) problem. The Mixed integer model, including the non-convex quadratic constraint, is efficiently solvable to global optimality by applying McCormick relaxations and spatial techniques as implemented in Gurobi solver (starting from version 9.1.2) to a MIPGap of 0.1%[25]. Constraint 66 includes three non-linear terms: Products of continuous and binary/Integer variables $H_t R_t^G$ and $R_t^{ES} R_t^G$ as well as the quadratic term $(P_t^L - R_t^{ES})^2$. McCormick lower and upper envelopes are applied to the products using auxiliary variables to linearise the bilinear terms in the nadir constraints[25]. Such that $H_t R_t^G$ is;

$$H_{t,l} R_t^G + R_{t,l}^G H_t \leq H_{t,l} R_{t,l}^G \tag{69}$$

$$H_{t,u} R_t^G + R_{t,u}^G H_t \leq H_{t,u} R_{t,u}^G \tag{70}$$

$$H_{t,u} R_t^G + R_{t,l}^G H_t \leq H_{t,u} R_{t,l}^G \tag{71}$$

$$H_{t,l} R_t^G + R_{t,u}^G H_t \leq H_{t,l} R_{t,u}^G \tag{72}$$

where $H_{t,l}, H_{t,u}, R_{t,l}^G, R_{t,u}^G$ are the lower and upper bounds of $H_t R_t^G$ respectively. The other products are linearised in similar manner and added to the model. The linearised coefficients and RHS of the McCormick constraints depend on variables' local bounds, which once changed, update the LP coefficients and RHS. The above constraints are then added via spatial branching techniques as locally valid cuts[25]. The spatial branching technique minimise the McCormick volume as much as possible[25]. The tighter McCormick relaxations replace weaker, more global ones, at local nodes leading to fewer simplex iterations, to support the solution of the transformed MILP problem. In addition, compared to other solvers, Gurobi delivers a globally valid lower bound on the optimal objective value by exploring the entire search space and with enough time through the tolerance, finds a globally optimal solution[25].

3.4 | PROBLEM FORMULATION FOR MODEL WITHOUT SCHEDULING CONSTRAINTS

In highlighting the benefits of detailed scheduling constraints in the proposed planning framework, this subsection presents a similar system design but with the classic clustered integer unit commitment formulations often adopted in research today. The planning framework was adapted to integrate a deterministic formulation of the mixed integer unit commitment constraints proposed by Reference[19,34]. The design mainly excludes the ramping and commitment constraints formulations for the single generators proposed in Section 3.1, Equation (30) - (42), which evaluates the flexibility of individual generators in the optimisation model. The formulation serves as a good baseline for comparison because it also includes the inertia-dependent post-fault frequency response requirements being adapted in the proposed model in the previous section. With the same constraints in Section 3.1 implemented, especially for other technologies like storage, hydrogen electrolysers, blue hydrogen, and renewable technologies, this section presents only key parts of the model that were modified according to where the clustered unit commitment variable, N^{up}_{t,n,g_T}, applies.

The problem formulation for the model without scheduling constraints is as follows:

$$V^O(x,\rho) := \sum_{b\in\Omega_B} w_b \sum_{t\in\Omega_T^b} \left\{ \tau_t \left[\sum_{g\in\Omega_G} c_g^G(P_{t,g}) + \sum_{n\in\Omega_N} \left[`\sigma^d_{t,n} + \sum_{s\in\Omega_S^n} (c_s^+ h_{t,s}^+ + c_s^- h_{t,s}^-) \right] \right] + \Upsilon R_t^{slack} + \sum_{g\in\Omega_G} c_{res} res_{t,g} + \sum_{g\in\Omega_G} c_{rsp} rsp_{t,g} \right\} \quad (73)$$

It is important to note that based on the model formulation in Reference[19,34], the operation cost objective function $V^O(x,\rho)$ in constraint (73) excludes the startup and shutdown costs. The generation limits[24,30] for this case which excludes detailed scheduling constraints, are as follows $\forall b \in \Omega_B, \forall t \in \Omega_T^b, \forall g \in \Omega_G := \Omega_N \times \Omega_G^T$

$$0 \le P_{t,g} + rsp_{t,g} + res_{t,g} \le (\overline{P}_g N^{up}_{t,n,g_T}) \quad (74)$$

The power output, frequency response and spinning reserve contributions of the clustered units are bounded by their maximum total amount of power output based on number of generators online N^{up}_{t,n,g_T} per time. We propose new linear constraints linking the operation of candidate generators g_T to the integer investment G_{n,g_T} to impose that a candidate generation unit can operate only if the necessary investment has taken place. In particular, the proposed constraints impose that the variables N^{up}_{t,n,g_T} can assume a nonzero value only if the generator g_T has been built. For all $b \in \Omega_B$, $\forall t \in \Omega_T^b$ and $g_T \in \Omega_G^T$ the following constraints,

$$N^{up}_{t,n,g_T} \le G_{n,g_T} \quad (75)$$

guarantee that a candidate generator can be active only if the relative investment has taken place. The ramp-up/down constraints for the clustered units are as follows $\forall b \in \Omega_B, \forall t \in \Omega_T^b - \{t_b^+\}, \forall g \in \Omega_G$

$$P_{t,g} - P_{t-1,g} + rsp_{t,g} + res_{t,g} \le RU_g \tau_t N^{up}_{t,n,g_T} \quad (76)$$

$$P_{t-1,g} - P_{t,g} \le RD_g \tau_t N^{up}_{t-1,n,g_T} \quad (77)$$

The thermal generators are also modelled to satisfy minimum up/down times and logical constraints, similar to constraints $(19-21)$. However. in this case $u_{t,g}$ is replaced with N^{up}_{t,n,g_T}. All the frequency response contribution from the clustered generation units $rsp_{t,g}$ are subject to physical limitations $\forall b \in \Omega_B$, $\forall t \in \Omega_T^b$, as in,

$$0 \le rsp_{t,g} \le \overline{Rsp}_g N^{up}_{t,n,g_T} \quad (78)$$

The largest power infeed P_t^L at time t is implemented such that,

$$\frac{P_{t,g}}{N^{up}_{t,n,g_T}} \le P_t^L \le P_L^{max}, \quad \forall g \in \Omega_G, i = 1, \ldots, Ng \quad (79)$$

This expression provides a non-linear expression of the decision variable P_t^L, given the need to optimise the largest loss of a single power production unit[19]. The expression was linearised using Big-M formulation and McCormick relaxation techniques, given that N^{up}_{t,n,g_T} is an integer decision variable[19]. The RoCoF, nadir and Steady-state security constraints used in this formulation are similar to constraints (57), (66) and (61).

However, the system inertia level after the largest generator loss is

$$H_t = \sum_{g\in\Omega_G} H_g \overline{P}_g N^{up}_{t,n,g} - P_L^{max} H_L. \quad (80)$$

These constraints were used to carry out further studies.

4 | METHODS AND TEST SYSTEM

The proposed model outlined above is applied to a single-node system to determine the generation (conventional, renewable and storage) mix for meeting system's different energy, frequency response and reserve requirements. The co-optimisation of investment and operation constraints led to a large number of constraints and variables in the model, shown in Table 1.

The numerical complexity of the problem and the large number of constraints and variables led to the decision to carry out this study first on a single-node system. The system does not assume any existing conventional generator types. Two candidate conventional generation technologies (H_2CCGT (HT), Nuclear

TABLE 1 Model components.

Model Components	Total Constraints	Quadratic Constraints	Bilinear Constraints
Number	4226902	672	1344
Total Variables	Continuous Variables	Integer Variables	Binary Variables
1915225	1436757	478468	470400

(NC), generators) investments are considered on a single node, with their parameters shown in Tables 2 and 3[28,35].

TABLE 2 Candidate Generator Data.

Type	p_g^{msg} (MW)	$\overline{P}_g$ (MW)	κ_g^G (\$/yr)	c_g^G (\$/MWh)	c_g^{su} (\$)
HT	500	500	54813.2.9	38	30780
Nc	1440	1800	530582.0	6	56710

TABLE 3 Technical thermal generators Data.

Type	H_g (s)	$\overline{Rsp}_g$ (MW)	T_g^{md} (h)	T_g^{mu} (h)	RU_g/RD_g (%$\overline{P}_g$/minute)
HT	4	85	4	4	60
Nc	5	0	4	4	1

Also, battery storage, renewable solar and wind generator technologies, electrolysers and hydrogen storage are part of the investment portfolio. The used renewable parameters are shown in Table 4.

TABLE 4 Candidate Renewable Generator Data.

No.	$R_{n,r}$ (MW)	κ_r^R (\$/yr)
Wind	6000	57565.77
Solar	1500	50261.2

The four seasons' (winter, spring, summer and autumn) wind and solar performance level factors have been extracted from GB historical data. Table 5 reports technical details for the storage. The Lithium Ion battery storage technology is modelled to have the capability of Enhanced Frequency response service provision delivered within T_s = 0.5s with $\overline{Rsp}_s = \overline{Res}_s$. The conventional generators provide PFR within T_g = 10s. Other parameters include D = 0.5%/Hz and P_L^{max} = 1800MW. The dynamic frequency requirements are set as in Reference[19].

TABLE 5 Candidate Storage Data.

$\overline{\eta}_s$	$\overline{h}_s$ (MWh)	ρ_s (MW)	κ_s^H (\$/yr)	c_s (\$/MW)	N_s^{res} (h)	N_s^{rsp} (h)
200	50	0.85	7650.76	5	4	0.5

The parameters for the blue and green hydrogen production (gas-heated reformers with carbon capture storage, GHR-CCS, and electrolysers, respectively), as well as storage technologies, are shown in Table 6 [28].

TABLE 6 Hydrogen Production and Storage technologies data.

Technology (o)	κ_o^H (\$/yr)	c_o (\$/MW)	η_o (%)
Electrolyser	36066.94	2.1	82%
Hydrogen Storage	520.05	0.149	99.67%
GHR-CCS	37222.43	61	61%

The hydrogen storage duration is 6 hours, while the conversion efficiency of H_2CCGT, η_{h2}, is 58.8%[28]. The marginal cost of GHR-CCS is higher, compared to electrolysers, due to the consideration of the carbon capture and storage for decarbonising the hydrogen fuel produced.

Demand profiles used on this system are based on representative historical typical days data from the Great Britain (GB) system. Four different week-long demand block profiles, representing all seasons of the year (winter, spring, summer and autumn) are considered, and the system's annual peak (electricity) demand is 71GW which totals to 167.9GW after including heat demand in the system[35]. This paper assumes that the heat sector will be decarbonised through electrification using heat pumps. Considering hydrogen demand, the amount of hydrogen is estimated by the model. However, the hydrogen production and storage modelling also considers an additional 123TWh hydrogen demand, with a profile modelled as flat, based industrial processes in a 2050 GB net-zero scenario[1,35].

The model was implemented in PYOMO[36,37] and solved with Gurobi Optimizer 10.0.0[25] on a High-Performance computer (HPC) with linux64, 128 physical cores, 256 logical processors, using up to 16 threads.

5 | RESULTS

Recalling that the research goal is to determine the influence of frequency response and detailed modelling of operational constraints in an integrated planning framework, a series of scenario studies were considered on the test system. The system settings common to all scenarios included:

- The Annual CO2 emissions target, E^T, was set to 0kg/MWh, representing the net-zero system.
- The generator scheduling constraints included the on/off status, minimum up/down time and start-up/shut-down trajectories of conventional generators.
- Battery storage was also modelled to provide flexibility in terms of energy arbitrage, spinning reserves and primary frequency response.

- The model was run with an hourly temporal resolution for one typical week per seasonal block at the operational level to determine the optimal power generation portfolio.

The obtained optimal generation mixes are analysed hereafter under different scenarios.

5.1 | Scenario Description

This subsection analyses the optimal technology portfolio mix with and without the modelling of detailed scheduling constraints for synchronous generators as constructed in Sections IV and VI, respectively. The case studies discussed in the section analyse the value of detailed scheduling constraints for synchronous generators like Hydrogen CCGT (H_2CCGT) fuelled by both blue and green hydrogen sources and moderately flexible nuclear plants (minimum stable generation set to 80% of its maximum capacity). Additional power generation technologies used in this scenario include renewable technologies (wind and solar plants). H_2CCGT, nuclear plants, and battery storage were modelled to provide spinning reserves, while imary frequency response (PFR) constraints were mostly delivered by battery storage and H_2CCGT.

This subsection also assesses the optimal technology portfolio mix considering frequency security constraints. We compare the optimal mix with and without frequency response requirements. Table 7 and 8 show the system's costs (Investment costs (IC), Operating costs (OC), Total costs (TC) in billion (bn) pounds/year) for the scenarios with and without detailed scheduling constraints, respectively. In both scenarios, similar studies on the impact of the frequency response constraints in the model were carried out and reported.

TABLE 7 Annual systems cost for Blue & Green hydrogen case with detailed scheduling constraints (Case A –All FR constraints included, Case B –Nadir constraints excluded, Case C –Nadir & Rocof constraints excluded, Case D –All FR constraints excluded)

Type	*CaseA*	*CaseB*	*CaseC*	*CaseD*
IC($bn/yr)	28.47	28.39	27.42	27.33
OC($bn/yr)	5.69	5.77	1.60	1.44
TC($bn/yr)	34.16	34.16	29.01	28.77

5.1.1 | Value of modelling detailed scheduling constraints

The value of modelling detailed scheduling constraints will be assessed by comparing systems cost of Case A and Case E reported in Tables 7 and 8, respectively. The systems cost in Tables 7 include detailed scheduling constraints, while Table 8 do not have detailed scheduling constraints. Case A, in Table 7. reports a higher systems cost (difference of £4.56bn/yr) based on higher investment and operation costs compared to

TABLE 8 Annual systems cost for Blue & Green hydrogen case without detailed scheduling constraints (Case E –All FR constraints included, Case F –Nadir constraints excluded, Case G –Nadir & RoCoF constraints excluded, Case H –All FR constraints excluded)

Type	*CaseE*	*CaseF*	*CaseG*	*CaseH*
IC($bn/yr)	27.74	27.75	27.76	27.73
OC($bn/yr)	1.84	1.83	1.36	1.32
TC($bn/yr)	29.59	29.59	29.12	29.05

Case E. A smaller difference (£73 million/yr) in investment cost is observed compared to the difference in operation costs (£3.9bn/yr), and the composition of the investment cost per technology is shown in Figure 2. Case E's almost similar investment portfolio reveals higher investment in wind plants, battery storage and hydrogen storage compared to Case A.

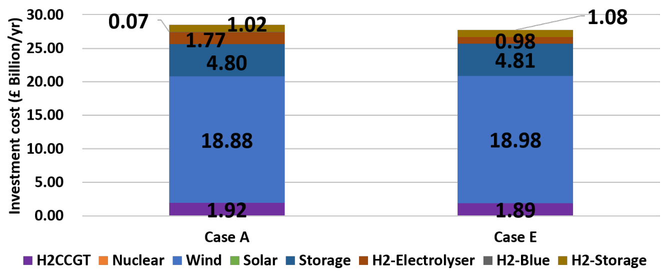

FIGURE 1 Investment cost per technology (Case A –Model with detailed scheduling constraints, Case E –model without detailed scheduling constraints)

Figure 2(a-d) emphasizes the differences between the capacity mixes and highlights reduced investment in blue and green hydrogen sources related to the reduction observed in H_2CCGT plants in Case E.

In a bid to understand the higher operation costs observed in Case A, the impacts of the detailed scheduling constraints are further assessed by fixing the technology investment solution of Case E as inputs for Case A. The simulation resulted in a total systems cost of £476.14bn/yr, with investment cost at £27.75bn/yr and operation costs at £443.33bn/yr, based on demand curtailments. The results reported in Figure 3 show the demand curtailment costs (£443.33bn/yr) and additional operation costs (£442.70bn/yr) to the system for meeting demand if technology investments were based on the model outputs without detailed scheduling constraints. The high curtailment cost was due to an annual demand curtailment of 14.78TWh and its high price (£30,000/MWh), shown in Figure 4 (a-b). The Figure also highlights that most of the curtailment occurs in winter during periods of significant variations in net demand when ramping constraints are critical. In particular, Figure 4(b)

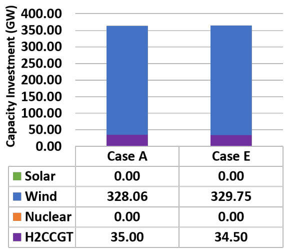

(a) Capacity Investment for power generating technologies

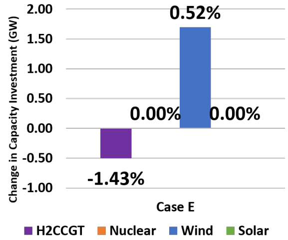

(b) Change in Capacity Investment against Case A

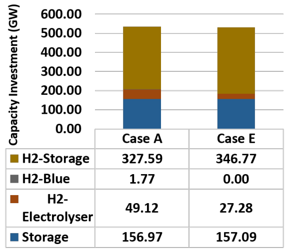

(c) Capacity Investment for flexible technologies

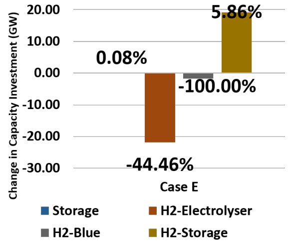

(d) Change in Capacity Investment against Case A

FIGURE 2 Capacity Investment of technologies for Blue –Green hydrogen case with vs without detailed scheduling constraints (Case A –Model with detailed scheduling constraints, Case E –model without detailed scheduling constraints)

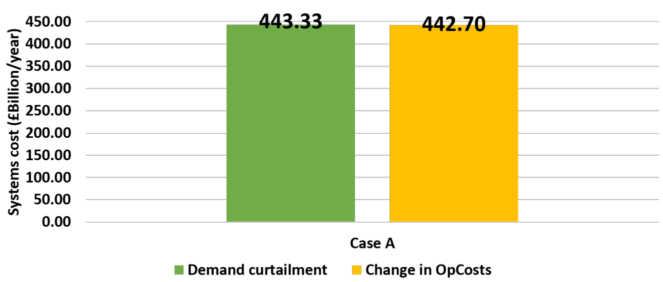

FIGURE 3 Demand curtailment & change in Operational cost for fixed investment solution(Case A –Model with detailed scheduling constraints

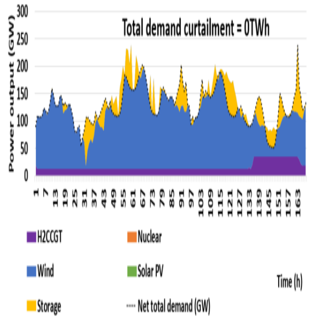

(a) Generation profile in Case A

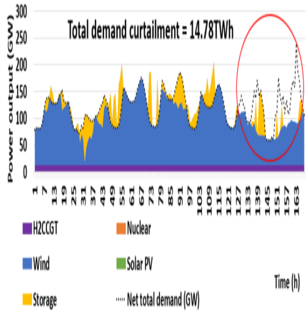

(b) Generation profile with solution for Case E fixed in Case A showing demand curtailment

FIGURE 4 Generation profile for typical winter week (Case A –Model with detailed scheduling constraints, Case E –model without detailed scheduling constraints)

shows that the H_2CCGT technologies did not ramp quickly enough during low wind and steep changes in net demand. The curtailment costs also led to the considerable change in operation costs observed in Figure 3. This disparity shows that even if the difference in system mix and cost is small, their ability to serve demand and satisfy constraints is very different.

5.1.2 | Value of modelling Frequency security constraints

Cases B-C in Table 7 and Cases F-H in Table 8 report the optimized costs with and without scheduling constraints under different assumptions on the frequency response requirements. In particular, Cases B and F neglect the nadir constraints (66), Cases C and G do not include nadir and ROCOF constraints (but the constraints on the system inertia and largest generator loss are present in the model) and Cases D and H exclude all the frequency response constraints are excluded. The systems' costs for Cases A and B reported in Table 7 are similar, but the operation and investment costs differ. In Case B, which excludes the nadir constraints, the operation cost decreased by 1.39% and the investment cost increased by 0.28% compared to Case A, as shown in Figure 5. However, removing both the nadir and ROCOF constraints in Case C led to a 71.94% and 3.69% decrease in operations and investment costs, respectively. In Case C, the system inertia constraints 59 were included in the model. The inertia constraints are excluded in Case D, which led to a 74.61% and 4.01% decrease in operation and investment costs, respectively. The differences in the systems cost account for the additional flexibility needed for system security and stability [19].

Figure 5 also shows how the PFR constraints impact the solution when neglecting the detailed modelling of the scheduling constraints, using Case A as the base case. The removal of the PFR constraints in the manner described above shows a greater reduction in systems cost, especially the operation costs, between cases B-D compared to cases F-H without detailed scheduling constraints in Figure 5. However, very small changes are seen when assessing the impact of the frequency response constraints on the investment costs between Case E-H. These minor differences in Case E-H emphasize the value of the detailed modelling of the scheduling constraints for identifying the actual impact of the frequency constraints.

Figure 6 shows the system costs if the optimal investment mix obtained in Case D, which neglects frequency response constraints, is used in Cases A-C. The demand curtailment costs and change in operating costs with and without nadir constraints

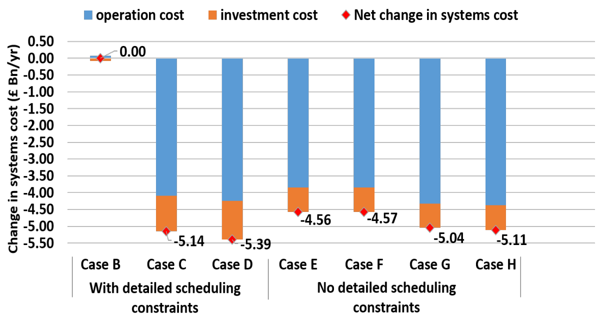

FIGURE 5 Change in systems cost for Blue & Green hydrogen case with vs without detailed scheduling constraints with respect to Case A (Case A –All FR constraints included, Case B –Nadir constraints excluded, Case C –Nadir & Rocof constraints excluded, Case D –All FR constraints excluded, Case E –All FR constraints included, Case F –Nadir constraints excluded, Case G –Nadir & RoCoF constraints excluded, Case H –All FR constraints excluded)

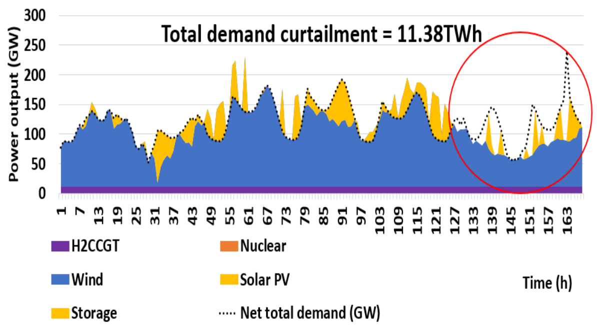

FIGURE 7 Generation profile in Case A for typical winter week when Case D investment solution is fixed in Case A and Case C (Case A –All FR constraints included, Case D –All FR constraints excluded)

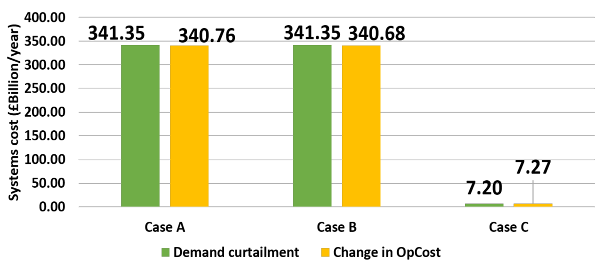

FIGURE 6 Demand curtailment & change in Operating costs using Case D solution(Case A –All FR constraints included, Case B –Nadir constraints excluded, Case C –Nadir & Rocof constraints excluded, Case D –All FR constraints excluded)

show similar high-cost effects of £341.35bn/yr and £340.7bn/yr, respectively. The high systems cost in Cases A and B show the criticality of including the ROCOF and nadir constraints in a system with unlimited enhanced frequency response from battery storage[23]. However, the demand curtailment costs and change in operations costs are much lower for Case C, where nadir and ROCOF constraints have been excluded. Figure 7 shows in detail the season demand curtailment occurs, which was mostly in the winter period, as previously described.

The impact of excluding the PFR constraints on the power generation and flexible technologies capacity investment mix with and without detailed scheduling constraints are shown in Figure 8. Figure 8 shows the changes in the power generation capacity mix (wind, nuclear and H_2CCGT) for Case A of cases with detailed scheduling constraints and without detailed scheduling constraints. Figure 8 also shows changes in flexible technologies like battery storage, H2-storage Blue, and green (electrolysers) hydrogen fuel sources. In Case B of Figure 8, there is a 0.8% decrease in wind capacity and a 1.43% increase in H_2CCGT capacity. There is a corresponding increase in hydrogen storage, blue and green hydrogen fuel with the increase in H_2CCGT plant capacity, while battery storage also increased slightly, as observed in Figure 8. However, excluding the ROCOF constraints in addition to the nadir constraints, Case C in Figure 8, resulted in a further decrease in wind plants capacity by 3.19% and a further increase in H_2CCGT capacity by 5.71%. On the contrary, it can be observed in Figure 8 that the increase in H_2CCGT was matched with a decrease in blue and green hydrogen fuel but an increase in battery and hydrogen storage, as observed.

An analysis of the annual generation profiles for Case C during the winter and spring week (Figure 9(a,b)) shows that H_2CCGT plants operate as peaking plants during critical periods of low wind generation and for a relatively short time (one or two days). The supply of large demand for short periods by H_2CCGT plants in a system with lower wind capacity, observed in Case C, compared to Cases A and B explains the increased investment in H_2CCGT and the further decrease in blue and green hydrogen, where H_2CCGT provided both baseload and part of the peak generation. Also, using the optimal investment mix obtained by neglecting the RoCoF constraints with RoCoF limitations reports a demand curtailment of 11.81TWh and consequently high costs of £354.39bn/yr.

Such demand curtailment represents the inadequacy of resource investments when nadir or RoCoF constraints are not considered in the planning phase. The changes in the technology investment mix in Case D, where all PFR security and inertia constraints are excluded, are similar to Case C but higher in percentage. The inadequacy of the technology investment mix obtained in Case D is highlighted in Figure 7, which reports substantial demand curtailment when frequency limitations must be satisfied.

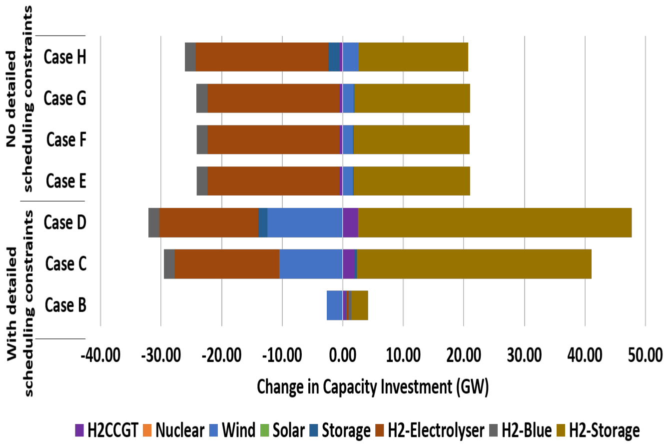

FIGURE 8 Change in capacity Investment of power and flexible generating technologies for Blue & Green hydrogen case with detailed scheduling constraints (Case A –All FR constraints included, Case B –Nadir constraints excluded, Case C –Nadir & Rocof constraints excluded, Case D –All FR constraints excluded, Case E –All FR constraints included, Case F –Nadir constraints excluded, Case G –Nadir & RoCoF constraints excluded, Case H –All FR constraints excluded)

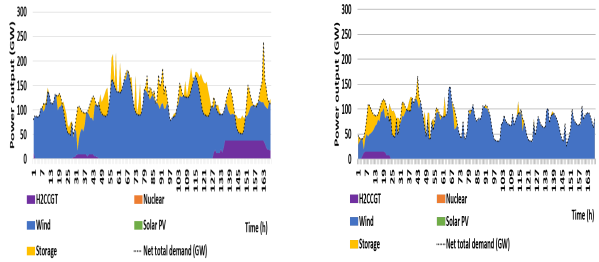

(a) Generation profile for a typical Winter week

(b) Generation profile for a typical Spring week

FIGURE 9 Generation profile in typical winter and spring week for Case C (Case C –Model with detailed scheduling constraints (Nadir & Rocof constraints excluded)

The percentage changes observed in Case E-H alternated such that investments in wind plants increased by 0.52% and H_2CCGT plant decreased by 1.43% based on excluding the detailed scheduling constraints. However, when comparing changes observed in Cases E-H in Figure 8 with changes in Cases A-D, the effect on the optimal mix induced by the frequency constraints is more evident considering detailed scheduling constraints. The investment capacity of wind and H_2CCGT plants are similar in Case E-G. The most significant change in the scenarios without detailed scheduling constraints was the 0.79% change in wind plants observed in Case H when all the frequency security constraints were excluded from the model. Figure 8 also shows that for Case E-H there is a corresponding increase in hydrogen storage capacity, while blue and green hydrogen fuel capacity decrease with the observed reduction in H_2CCGT plant capacity. However, there are no significant changes from excluding the frequency response constraints named in Case F-H. Similar to Case D, the greatest decrease in battery storage are observed in Case H when the frequency response constraints are excluded.

Figure 10 shows the share of annual generation output for the installed technologies when detailed modelling is included (Case A) and excluded (Case E), based on net demand on the system. The total generation output in Case A is 844.55TWh, while Case E is 657.39TWh. Even though the same system demand was used in both cases, the variation in their total generation output is mainly due to the flexible energy demand from the electrolysers used for hydrogen production. This flexible demand from the electrolyser is higher in Case A (13.05%), where the contribution from H_2CCGT to generation output is higher compared to Case E (2.69%). The high contribution of H_2CCGT in Case A is due to the detailed scheduling constraints, which depict the actual requirement of flexible generation on the system. However, wind plants deliver the highest percentage of annual generation output in both cases. Battery storage also contributes to the energy supply in both cases. In Case A, the charge-discharge activity of battery storage was summed and resulted in a net contribution of 1.22%, discharging more times than it charges. Whereas in Case E, the net contribution of battery storage is -2.32%, charging more times than it discharges.

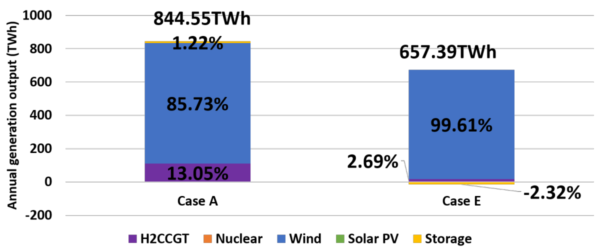

FIGURE 10 Share of Annual generation output (Case A –Model with detailed scheduling constraints, Case E –model without detailed scheduling constraints)

Figure 11 and 13 compare the spinning reserve and the primary frequency response provision mix in Case A and Case E. In particular, Figure 11 shows that H_2CCGT and battery storage technology meet all the spinning reserves requirements, with batteries having the largest share. Given that the reserve requirement, Res_t^{min}, is calculated as a percentage of system demand and renewable generation per time, the reserve requirement in Case E (148TWh) is higher compared to Case A (133TWh) due to higher investment in wind plant capacity observed in Figure 8. As a result, Case E shows a higher proportion of battery storage usage and H_2CCGT, respectively, for spinning reserve provision compared to Case A. Figure 12 provides further explanation for the results observed as it depicts the hourly scheduling of reserves in Case A and E. The results show that in Case E, the technologies, especially storage, are scheduled in excess for reserves provision compared to Case A. The detailed modelling of the scheduling constraints eliminates the overestimation of reserves from the different technologies.

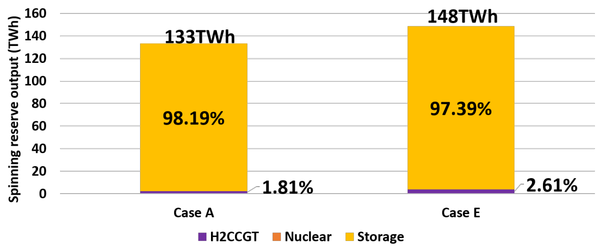

FIGURE 11 Share of Annual Spinning Reserve portfolio (Case A –Model with detailed scheduling constraints, Case E –model without detailed scheduling constraints)

A comparison of the Primary frequency reserve (PFR) portfolio in Figure 13, shows Case A and Case E are almost similar (circa. 16TWh) based on the requirement estimated from the size of the largest generator loss (P_t^L). In both cases, battery storage mostly provided frequency response, given its enhanced and faster frequency response capability compared to H_2CCGT. However, the contribution of H_2CCGT capacity in Case E (0.79TWh) was slightly higher compared to Case A (0.74TWh). The higher availability of H_2CCGT in Case E can be linked to the reduced use of H_2CCGT for meeting energy demand, as observed in Figure 10.

6 | DISCUSSION

Energy system models, especially investment planning models, are required for decision-making and to provide insights to energy stakeholders on key technologies valuable for achieving

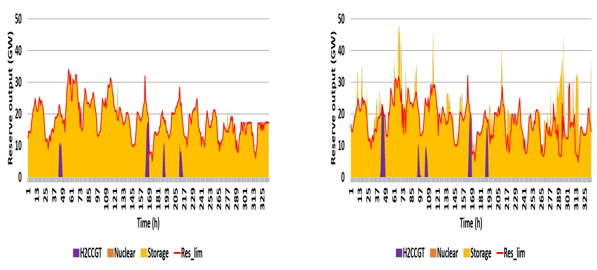

(a) Case A (b) Case E

FIGURE 12 Spinning Reserve profile for a typical combined winter and spring week (Case A –Model with detailed scheduling constraints, Case E –model without detailed scheduling constraints)

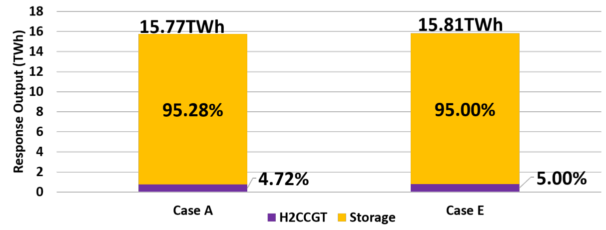

FIGURE 13 Share of Annual PFR portfolio (Case A –Model with detailed scheduling constraints, Case E –model without detailed scheduling constraints)

energy transition and decarbonisation targets. The proposed novel formulation and the case studies emphasize the importance of using an enhanced whole system model, which includes frequency requirements and detailed operational dynamics to support decision-making by policymakers, systems operators, utilities and investors.

The results of modelling detailed scheduling constraints in the proposed planning framework demonstrate that such modelling significantly impacts investment outcomes. The system cost increases to allow the system to edge against frequency variations. Specifically, the modelling ensured appropriate estimation of the capacity of technologies needed to support the required system flexibility in a low carbon future, and these were seen in the total capacity requirements for reserves and frequency response [32]. The changes observed were increased investment capacity in H_2CCGT plants, as well as blue and green hydrogen production technologies needed to fulfil the energy requirements in a net zero system, compared to a model without the detailed representation of the scheduling constraints. Despite an observed reduction in investments in wind plants, the investments in these hydrogen technologies are also required to support the integration of renewable technologies, especially for managing periods of variable and low renewable generation [2]. Investments in battery and hydrogen storage capacity are directly related to investments in renewable technologies, such as the reduction in wind plants, which reduced the amount of storage capacity required to support the technology [38]. The significance of these changes is that high curtailment costs of up to £443.33bn/yr were avoided when capacity planning was done using the outcomes of a model excluding the detailed modelling of unit commitment constraints and the ramping capability of individual generators units in a cluster.

Similarly, modelling the different frequency security constraints in an investment planning framework aids systems operators in accurately estimating investments in flexible technologies needed to support the system during a frequency round-trip [10]. By layering frequency security constraints on the detailed scheduling constraints in the model, it was demonstrated that modelling frequency constraints support the integration of renewable technologies into the system, leading to increased investments in wind plant capacity. These changes were evident because of the ramping capability of individual generation units captured in the model. It was also realised that compared to a model without any of the frequency response constraints, reduced capacity of H_2CCGT and hydrogen storage technologies are actually needed for supporting the system's flexibility. In addition, it was demonstrated that increased investment in battery storage was required to manage the frequency changes in the system based on its fast response. Considering nadir constraints and requirements at planning level contributes to driving better investment decisions for managing near under-frequency load shedding situations. As shown in the case study, not considering nadir constraints at the planning level can cause very high curtailment costs of up to £340bn/yr , no security of supply and reduced demand - supply balancing.

Even though the model can integrate a dynamic power in-feed loss, this study assumed the loss of the largest generator, which is a nuclear plant included in the technology mix. Sensitivity analysis on a dynamic power in-feed loss which could vary from the actual power output of a power production unit to the maximum power output of the largest generator as seen in equations (55) and (56) were not carried out, but the author anticipates it would lead to significant changes in the investment planning outcomes. Moreover, by modelling these complex constraints and the interactions between electricity and hydrogen vectors, the framework provided insights of the interactions between these energy vectors and managed the possibility of overestimating or underestimating the actual capacity of flexible technologies required to support the system in the integration of low carbon technologies and during diverse operational challenges[32]. This was specifically observed in changes in the capacity investments for wind, H_2CCGT plants, blue and green hydrogen plants, and hydrogen storage when the additional constraints were integrated.

6.1 | Computation Time

The detailed modelling approach increased the computational complexity of the model, as highlighted by the number of constraints and variables highlighted in Table 1. The large number of constraints and variables greatly impacted the computation (CPU) time as the deterministic mixed integer quadratic programming model solved in the range of time shown in Table 9. Compared to the model without the detailed scheduling constraints, the model with detailed scheduling constraints required a CPU time of 16h 30m to solve to optimality (0.001% Gap). The computation time is reduced by approximately 1h when removing any of the frequency security constraints. Moreover, the model's performance shows the detailed scheduling constraints largely impact the computation time. This computational performance highlights great consideration would need to be given to the trade-off between achieving a more accurate estimate of investment results and the amount of time required to solve such a model to optimality.

TABLE 9 Model Computation time.

Model	CPU time	Relative Gap
Model without scheduling constraints	10s	0.00%
Model with scheduling constraints	16h 30m	0.00%
Model without nadir constraints	15h 19m	0.00%
Model without Frequency security constraints	14h 17m	0.00%

MIP problems are generally NP-hard, but this model has been enhanced with tight and compact detailed unit commitment constraints and additional constraints removing the symmetries due to the potential presence of multiple identical generators. Experimental testing, as shown in the reported studies, demonstrates the model performs well, reducing the likelihood of overestimating the investment solution.

7 | CONCLUSION

This paper investigates the impact of detailed frequency stability and mixed integer unit commitment constraints, amongst other operational details, on a power system planning problem. A novel integrated planning framework was proposed to identify optimal technology portfolios for a cost-effective electricity system while ensuring frequency stability and reserve requirements. The studies concurrently optimized investments in low-carbon technologies while minimizing the system's short-term operating costs through hourly time resolution representation of the system operation alongside reserve, frequency stability and regulation requirements for a net-zero Great Britain system. The outcome of the studies highlighted the importance of detailed operational constraints for accurately estimating the optimal low-carbon technologies needed in a net-zero system. The results obtained provided optimal and significant trade-offs and cost-effective investment portfolios, from including detailed modelling of unit commitment scheduling and frequency stability constraints versus not including them in a power systems planning problem. The trade-offs were observed in the increased system's costs, based on additional investment in flexible technologies, especially H_2CCGT plants, battery storage, and other hydrogen production and storage technologies required to manage the system should any operational challenges such as the loss of the largest generator, occur. The results also emphasized that the system can experience higher annual total costs than anticipated due to high demand curtailment by making investment decisions without considering frequency constraints and a detailed unit commitment. The curtailments were observed during periods of low wind generation and when the system required quick ramping response from flexible power generators. The studies showed that an investment planning framework without frequency security constraints for managing frequency imbalance and detailed modelling of the unit commitment scheduling constraints would lead to resource inadequacy and an underestimation of the technology portfolio required in a net zero system.

Future work will involve further investigation of the trade-offs and optimal portfolio based on modelling emerging technologies, which can support the flexibility needs of low-carbon power systems in terms of frequency response, systems inertia, and spinning reserve. In addition, future work will include actual grid networks and consider spatial frequency variability and network security constraints. The study will also evolve to carry out a stochastic analysis based on introducing short-term uncertainties in renewable generation or demand. With the solution of this scale of framework being very complex, uncertainty sources can be considered by adding robust margins to different system requirements like the spinning reserve and frequency response requirements, similarly employed by Reference[39]. Another example of an uncertainty source is to add a reserve margin to the generator loss P_t^L estimated by considering the statistical property of a variable generator loss. Using robust margins introduces conservativeness when considering uncertainties but in complex models it is inevitable. Future works will also include conducting sensitivity analysis on using a dynamic power in-feed loss compared to a fixed power in-feed loss.

AUTHOR CONTRIBUTIONS

Olayinka Ayo: Conceptualization, research, methodology, Software, Analysis, Writing, review editing; **Paola Falugi**: Conceptualization, methodology, review editing, Supervision; **Goran Strbac**: Methodology, Review editing, Supervision.

ACKNOWLEDGMENTS

Olayinka Ayo would like to acknowledge the Petroleum Development Fund (PTDF) for their funding of the research.

CONFLICT OF INTEREST

The authors declare no potential conflict of interests.

REFERENCES

1. Climate Change Committee oC. The Sixth Carbon Budget: The UK's path to Net Zero. tech. rep., Report; 2020.
2. Strbac G, Pudjianto D, Aunedi M, et al. Role and value of flexibility in facilitating cost-effective energy system decarbonisation. *Progress in Energy.* 2020;2(4):042001.
3. Strbac G, Konstantelos I, Pollitt M, Green R. Delivering future-proof energy infrastructure Report for. *National Infrastructure Commission.* 2016(February):54.
4. Grid N. Future Energy Scenarios. *Report.* 2020.
5. Strbac G, Pudjianto D, Druce R, Borkowski K. Value of Flexibility in a Decarbonised Grid and System Externalities of Low-Carbon Generation Technologies For the Committee on Climate Change NERA Project Team :. Tech. Rep. October, Imperial College; London: 2015.
6. Zhang X, Strbac G, Shah N, Teng F, Pudjianto D. Whole-System Assessment of the Benefits of Integrated Electricity and Heat System. *IEEE Transactions on Smart Grid.* 2019;10:1132–1145.
7. Pudjianto D, Aunedi M, Djapic P, Strbac G. Whole-systems assessment of the value of energy storage in low-carbon electricity systems. *IEEE Transactions on Smart Grid.* 2014;5:1098–1109.
8. Paturet M, Markovic U, Delikaraoglou S, Vrettos E, Aristidou P, Hug G. Stochastic Unit Commitment in Low-Inertia Grids. *arXiv preprint arXiv:1904.03030.* 2019.
9. Baik E, Chawla KP, Jenkins JD, et al. What is different about different net-zero carbon electricity systems?. *Energy and Climate Change.* 2021;2:100046.
10. Helistö N, Kiviluoma J, Morales-España G, O'Dwyer C. Impact of operational details and temporal representations on investment planning in energy systems dominated by wind and solar. *Applied Energy.* 2021;290:116712.
11. Schwele A, Kazempour J, Pinson P. Do unit commitment constraints affect generation expansion planning? A scalable stochastic model. *Energy Systems.* 2020;11(2):247–282.
12. Morales-España G, Baldick R, García-González J, Ramos A. Power-capacity and ramp-capability reserves for wind integration in power-based UC. *IEEE Transactions on Sustainable Energy.* 2015;7(2):614–624.
13. Tejada-Arango DA, Morales-España G, Wogrin S, Centeno E. Power-Based Generation Expansion Planning for Flexibility Requirements. *arXiv preprint arXiv:1902.07779.* 2019.
14. Tejada-Arango DA, Lumbreras S, Sánchez-Martín P, Ramos A. Which Unit-Commitment Formulation is Best? A Comparison Framework. *IEEE Transactions on Power Systems.* 2019;35(4):2926–2936.
15. Poncelet K, Delarue E, D'haeseleer W. Unit commitment constraints in long-term planning models: Relevance, pitfalls and the role of assumptions on flexibility. *Applied Energy.* 2020;258:113843.
16. Morales España GA, Tejada Arango DA. Modelling the hidden Flexibility of clustered unit commitment. 2019.
17. National Grid . System Needs and Product Strategy. Tech. Rep. June, National Grid Plc; Warwick: 2017.
18. Aurecon . Hornsdale Power Reserve: Year 1 Technical and Market Impact Case Study. tech. rep., Australia: 2018.
19. Badesa L, Teng F, Strbac G. Simultaneous Scheduling of Multiple Frequency Services in Stochastic Unit Commitment. *IEEE Transactions on Power Systems.* 2019:1–11.
20. Teng F, Strbac G. Understanding of the Flexibility from Combined Cycle Gas Turbine Plant. In: Badescu V, Lazaroiu GC, Barelli L., eds. *Power Engineering: Advances and Challenges, Part A: Thermal, Hydro and Nuclear Power*, , Taylor and Francis Group, 2018:26.
21. Wogrin S, Tejada-Arango D, Delikaraoglou S, Botterud A. Assessing the impact of inertia and reactive power constraints in generation expansion planning. *Applied Energy.* 2020;280:115925.
22. Kushwaha P, Prakash V, Bhakar R, Yaragatti UR, Jain A, Sumanth Y. Assessment of Energy Storage Potential for Primary Frequency Response Adequacy in Future Grids. *2018 8th IEEE India International Conference on Power Electronics (IICPE).* 2018:1–6.
23. Gonzalez-Longatt F, Roldan-Fernandez JM, Chamorro HR, Arnaltes S, Rodriguez-Amenedo JL. Investigation of Inertia Response and Rate of Change of Frequency in Low Rotational Inertial Scenario of Synchronous Dominated System. *Electronics.* 2021;10(18):2288.
24. G. Morales-España JML, Ramos A. Tight and Compact MILP Formulation for the Thermal Unit Commitment Problem. *IEEE Transactions on Power Systems.* 2013;28:4897–4908.

25. Gurobi Optimization L. Gurobi optimizer reference manual. 2021.
26. Sepulveda NA, Jenkins JD. Enhanced Decision Support for a Changing Electricity Landscape: the GenX Configurable Electricity Resource Capacity Expansion Model. *In Preparation for Publication.* 2017:1–40.
27. Moreira A, Street A, Arroyo J. Energy and reserve scheduling under correlated nodal demand uncertainty: An adjustable robust optimization approach. *International Journal of Electrical Power and Energy Systems.* 2015;72:91–98.
28. Fu P, Pudjianto D, Zhang X, Strbac G. Integration of Hydrogen into Multi-Energy Systems Optimisation. *Energies.* 2020;13(7):1606.
29. Garifi K, Baker K, Christensen D, Touri B. Convex relaxation of grid-connected energy storage system models with complementarity constraints in DC OPF. *IEEE Transactions on Smart Grid.* 2020;11(5):4070–4079.
30. Gentile C, España GM, Ramos A. A tight MIP formulation of the unit commitment problem with start-up and shut-down constraints. *EURO J. Comput. Optim..* 2016.
31. Teng F, Trovato V, Strbac G. Stochastic Scheduling With Inertia-Dependent Fast Frequency Response Requirements. *IEEE Transactions on Power Systems.* 2016;31:1557–1566.
32. Helistö N, Kiviluoma J, Holttinen H, Lara JD, Hodge BM. Including operational aspects in the planning of power systems with large amounts of variable generation: A review of modeling approaches. *Wiley Interdisciplinary Reviews: Energy and Environment.* 2019;8(5):e341.
33. Collins S, Deane JP, Gallachóir BÓ. Adding value to EU energy policy analysis using a multi-model approach with an EU-28 electricity dispatch model. *Energy.* 2017;130:433–447.
34. Teng F, Trovato V, Strbac G. Stochastic scheduling with inertia-dependent fast frequency response requirements. *IEEE Transactions on Power Systems.* 2015;31(2):1557–1566.
35. Lever A, Evans H, Ravishankar M, et al. Flexibility in Great Britain. 2021.
36. Hart WE, Laird CD, Watson JP, et al. *Pyomo–optimization modeling in python*. 67. Springer Science & Business Media, 2017.
37. Hart WE, Watson JP, Woodruff DL. Pyomo: modeling and solving mathematical programs in Python. *Mathematical Programming Computation.* 2011;3(3):219–260.
38. Strbac G, Pudjianto D, Sansom R, et al. Analysis of alternative UK heat decarbonisation pathways. *Imperial College London: London, UK.* 2018.
39. Sturt A, Strbac G. Efficient stochastic scheduling for simulation of wind-integrated power systems. *IEEE Transactions on Power Systems.* 2011;27(1):323–334.

APPENDIX

A NOMENCLATURE

This section introduces the mathematical symbols most recurrently used in the article.

A.0.1 Sets

Ω_B Set of demand blocks indexed by b.

Ω_N Set of system nodes indexed by n.

Ω_G^T Set of conventional generation technologies indexed by g_T.

Ω_G Set $\Omega_N \times \Omega_G^T$ of clusters associated to node n and technology g_T indexed by $g = (n, g_T)$.

N_g Number of generator within a cluster g.

Ω_I^g Set of generation units in the cluster $g \in \Omega_G$ indexed by i

Ω_T^b Set of time periods in demand block b indexed by t.

Ω_R^T Set of candidate renewable technologies.

Ω_R Set of all renewables indexed by r.

Ω_S Set of all storage technologies indexed by s.

Ω_S^E Subset of electricity storage technologies ($\Omega_S^E \subseteq \Omega_S$) indexed by es.

Ω_S^H Subset of H_2 storage technologies ($\Omega_S^H \subseteq \Omega_S$) indexed by hs.

Ω_{EL}^T Set of electrolyser candidate technologies.

Ω_{BL}^T Set of blue hydrogen candidate technologies.

A.0.2 Parameters

$d_{t,n}$ Demand (MW) at node n and time t.

$I_{n,\ell}$ Bus-to-line incidence matrix of size $|\Omega_N| \times |\Omega_L|$.
$I_{n,\ell} = 1$ if line ℓ is from the sending bus node n
$I_{n,\ell} = -1$ if line ℓ is from the receiving bus node n
$I_{n,\ell} = 0$ otherwise

$\tilde{h}_s^0$ Initial state-of-charge of storage device s.

$J_{n,g}$ Bus-to-generation cluster incidence matrix ($|\Omega_N| \times |\Omega_G|$).
$J_{n,g} = 1$ if generator g connects to bus n
$J_{n,g} = 0$ otherwise

$\overline{h}_{es}$ Maximum charge/discharge rate (MW) of storage es.

ρ_{es} Charging/discharging efficiency of storage es.

N_g Maximum number of generator units within cluster g.

$\overline{P}_g$ Maximum power output (MW) of a conventional generator unit g.

$\overline{G}_{n,g_T}$ Maximum number of investments in conventional generators of technology g_T at bus node n.

p_g^{msg} Minimum stable generation (MW) of cluster unit g.

` System balance penalty constant (\$/MWh).

ˇ Reserve penalty constant (\$/MWh).

κ_o^ℓ Annual fixed capital cost (\$/(km yr)) of line ℓ, option o.

κ_r^R Annual capital cost (*\$/yr*) of renewable technology r.

κ_{es}^H Annual capital cost (*\$/yr*) of storage devices es.

κ_g^G Annual capital cost (*\$/yr*) of generator cluster unit g.

κ_{el}^H Annual capital cost (*\$/yr*) of electrolyser units el.

κ_{hs}^H Annual capital cost (*\$/yr*) of hydrogen storage units hs.

c_g^{su} Startup cost (\$) of generator cluster unit g.

c_g^{sd} Shutdown cost (\$) of generator cluster unit g.

c_g^{nl} No-load cost (*\$/h*) of generator cluster unit g.

c_g^G Operation cost (*\$/MWh*) of generator cluster unit g.

c_s^- Discharging cost (*\$/MWh*) of storage unit s.

c_s^+ Charging cost (*\$/MWh*) of storage unit s.

c_{hs}^- H_2 consumption cost (*\$/MW*) of storage unit hs.

c_{hs}^+ H_2 production cost (*\$/MW*) of storage unit hs.

c_{el} H_2 production cost (*\$/MW*) by electrolyser unit el.

c_{bl} H_2 production cost (*\$/MW*) by blue H_2 unit bl.

c_{res} Cost (*\$/MW*) of reserve scheduling.

T_g^{md} Minimum down time (h) of generator cluster unit g.

T_g^{mu} Minimum up time (h) of generator cluster unit g.

$\overline{\eta}_{es}$ Energy capacity (*MWh*) of storage es.

η_{el}	Conversion efficiency of the electrolyser *el*.
η_{hs}	Conversion Efficiency of H_2 storage *hs*.
η_{h2}	Conversion efficiency of the H_2CCGT.
RU_g	Ramp-up limit (MW/h) of unit g.
RD_g	Ramp-down limit (MW/h) of unit g.
$\hat{S}^{-}_{es}$	Total discharge capacity (MW) of storage *es*.
SU_g	Start-up capability (MW) of generator cluster unit g.
SD_g	Shut-down capability (MW) of generator cluster unit g.
w_b	weight of demand block b.
t^{+}_{b}	First period of demand block b.
t^{-}_{b}	Last period of demand block b.
E^T	Annual emission limit (kg/MWh).
Δf_{max}	Maximum admissible frequency deviation.
Δf^{ss}_{max}	Maximum quasi-steady state frequency deviation.
D	Load-damping factor ($\%Hz$).
f_0	Nominal frequency (Hz) of the power grid.
H_g	Inertia constant (s) of generator cluster units g.
H_L	Inertia constant (s) of generator producing P^L_t.
P^{max}_{L}	Bound of the largest power infeed (MW).
$\overline{RoCoF}$	Maximum admissible RoCoF (Hz/s).
T_g	Delivery time (s) of PFR.
T_{es}	Delivery time (s) of EFR.
P^D_t	Total demand (MW) at time t.
Δ^{hs}_{t}	H_2 storage duration (hours).
Δf_{nadir}	Frequency at nadir in Hz.
$h^{+}_{t,n,hs}$	H_2 production by H_2 storage *hs* at bus n and time t.
$h^{-}_{t,n,hs}$	H_2 consumed by H_2 storage *hs* at bus n and time t.
$\tilde{h}_{t,n,hs}$	Energy content of H_2 storage *hs* at bus n and time t.
$rsp_{t,g}$	Frequency response provided by cluster generator g (MW) at time t.
$\tilde{rsp}_{t,g,i}$	Frequency response provided by generator unit i in cluster g at time t.
$res_{t,g}$	Spinning reserve provided by cluster generator g (MW) at time t.
$\tilde{res}_{t,g,i}$	Spinning reserve provided by generator i in cluster g (MW) at time t.
$u_{t,g}$	Integer variable for commitment of number of generator units in cluster g at time t.
$\tilde{u}_{t,g,i}$	Binary variable of unit i in cluster g at time t. It is 1 if unit i is producing above minimum output and 0 otherwise.
$u^{+}_{t,g}$	Startup of unit g at time t. it takes 1 if unit starts up at time t and 0 otherwise.
$u^{-}_{t,g}$	Shutdown of unit g at operating point t. it takes 1 if unit shuts down at time t and 0 otherwise.
$\hat{\alpha}^{rsp}_{es,t}$	Proportion of storage charging that can be interrupted to provide frequency response.
$\hat{\alpha}^{res}_{es,t}$	Proportion of storage charging that can be interrupted to provide operating reserves.
R^{slack}_{t}	Reserve curtailment (MW) at operating point t.
P^L_t	Largest power infeed (MW) at time t.
H_t	System inertia (MWs) after the loss of P^L_t.
R^G_t	Total PFR (MW) from all generators.
R^{ES}_t	Total EFR (MW) from all storage units.

A.0.3 Decision Variables

All decision variables, denoted as x, are as follows:

G_{n,g_T}	Candidate (integer) generators of technology g_T at bus n.
$H_{n,es}$	Candidate storage *es* at bus n.
$R_{n,r}$	Candidate renewable technology r at bus node n.
$G^H_{n,el}$	Candidate electrolyser *el* at bus n.
$G^H_{n,bl}$	Candidate blue H_2 technologies *bl* at bus n.
$\overline{S}_{n,hs}$	Candidate H_2 storage *hs* at bus n.
$p_{t,g}$	Cluster generator power output (MW) at time t.
$\tilde{p}_{t,g,i}$	Power output (MW) above minimum output of generator unit i in cluster g at time t.
$P_{t,g}$	Total cluster generator power output (MW) at time t.
$Q_{t,n,el}$	Green H_2 production (MW) at time t.
$Q_{t,n,bl}$	Blue H_2 production (MW) at time t.
$p^R_{t,n,r}$	Power output (MW) of renewable r at bus n and time t.
$f_{t,\ell}$	Power flow in line ℓ at time t.
$\theta_{t,n}$	Bus angle at node n and time t.
$h^{+}_{t,es}$	Power charge of storage *es* at time t.
$h^{-}_{t,es}$	Power discharge of storage *es* at time t.
$\tilde{h}_{t,es}$	State of charge of storage *es* at time t.